The C+N+O abundance of ω Centauri giant stars: implications on the chemical enrichment scenario and the relative ages of different stellar populations [1]

A. F. Marino[1], A. P. Milone[2,3], G. Piotto[4], S. Cassisi[5], F. D'Antona[6], J. Anderson[7], A. Aparicio[2,3], L. R. Bedin[8], A. Renzini[8], S. Villanova[9]

[1]Max-Planck-Institut für Astrophysik, Karl-Schwarzschild-Str. 1, 85741 Garching bei München, Germany

`amarino@MPA-Garching.MPG.DE`

[2]Instituto de Astrofísica de Canarias, E-38200 La Laguna, Tenerife, Canary Islands, Spain

`milone@iac.es, aparicio@iac.es`

[3]Departamento de Astrofísica, Universidad de La Laguna, E-38200 La Laguna, Tenerife, Canary Islands, Spain

[4]Dipartimento di Astronomia, Università di Padova, Vicolo dell'Osservatorio 3, Padova, I-35122, Italy

`giampaolo.piotto@unipd.it`

[5]INAF-Osservatorio Astronomico di Teramo, Via M. Maggini, 64100 Teramo, Italy

`cassisi@oa-teramo.inaf.it`

[6]INAF-Osservatorio Astronomico di Roma, via Frascati 33, I-00040 Monteporzio, Italy

`dantona@oa-roma.inaf.it`

[7]Space Telescope Science Institute, 3700 San Martin Drive, Baltimore, MD 21218, USA

`jayander@stsci.edu`

[8]INAF-Osservatorio Astronomico di Padova, Vicolo dellOsservatorio 5, 35122 Padova, Italy

`luigi.bedin@oapd.inaf.it, alvio.renzini@oapd.inaf.it`

[9]Departamento de Astronomía, Universidad de Concepción, Casilla 160-C, Concepción, Chile

ABSTRACT

We present a chemical-composition analysis of 77 red-giant stars in Omega Centauri. We have measured abundances for carbon and nitrogen, and combined our results with abundances of O, Na, La, and Fe that we determined in our previous work. Our aim is to better understand the peculiar chemical-enrichment history of this cluster, by studying how the total C+N+O content varies among the different-metallicity stellar groups, and among stars at different places along the Na-O anticorrelation. We find the (anti)correlations among the light elements that would be expected on theoretical ground for matter that has been nuclearly processed via high-temperature proton captures. The overall [(C+N+O)/Fe] increases by ∼0.5 dex from [Fe/H]∼ −2.0 to [Fe/H]∼ −0.9. Our results provide insight into the chemical-enrichment history of the cluster, and the measured CNO variations provide important corrections for estimating the relative ages of the different stellar populations.

Subject headings: globular clusters: individual (NGC 5139) —

1. Introduction

Omega Centauri (ω Cen) is one of the most intriguing Globular Clusters (GCs) of the Galaxy. At odds with the majority of GCs, which are mono-metallic, it shows large star-to-star metallicity variations up to more than one dex (e.g. Norris, Freeman & Mighell 1996, Suntzeff & Kraft 1996). At the same time, it shares with the most mono-metallic GCs the presence of a Na-O anticorrelation, which is present across almost the entire metallicity range (Marino et al. 2011a, Johnson & Pilachowski 2010). These two facts suggest unique complexity in the cluster's star-formation history, and its chemical evolution.

The complexity of ω Cen also manifests itself in its color-magnitude diagram (CMD) with the presence of multiple red-giant (RGBs), multiple sub-giant branches (SGBs, Lee

svillanova@astro-udec.cl

et al. 1999, Pancino et al. 2000), and an extended horizontal branch (Villanova et al. 2007; Cassisi et al. 2009, D'Antona, Caloi & Venura 2010; Bellini et al. 2010). The main sequence (MS) is double (Anderson 1997), and a third, less-populated MS has been discovered by Bedin et al. (2004) and associated with the most metal-rich population. The bluer MS (bMS) has a higher metallicity than the red MS (rMS, Piotto et al. 2005). So far, the only way to account for these observations is to assume the bMS to be highly enhanced in He (Norris 2004; Bedin et al. 2004; Piotto et al. 2005). Direct evidence in this directions has been recently detected from the analysis of the He I 10830 transition on ω Cen RGB stars (Dupree et al. 2011). The correlation of the He line detection with [Fe/H], Al and Na supports the assumption that helium is enhanced in the bMS.

Due to the observational scenario, more complex than in any other GC, it has often been suggested (e.g. Bekki & Freeman 2003) that ω Cen may be the remnant of a now-dissolved dwarf galaxy, once similar of the Sagittarius dwarf (with its central globular cluster M54) now being thorn apart by the Galactic tidal field. In any case, a successful description of the ω Cen star-formation history should be able to explain both the Na-O anticorrelation at the various metallicities and the general rise in slow-process (s-process) elements as a function of metallicity (Norris & Da Costa 1995; Johnson & Pilachowski 2010; Smith et al. 2000; Marino et al. 2011a). The presence of the Na-O anticorrelation implies that ω Cen, similarly to mono-metallic GCs, has experienced enrichment from high-temperature H-burning processed material. At the same time, an additional physical mechanism should be present to produce s-process elements. In the Sun, the s-process elements abundance is mainly due to two components: the main component (attributed to low-mass AGB stars of 1.5-3M$_\odot$; Busso, Gallino & Wasserburg 1999) and the weak component (attributed to massive stars; see Raiteri et al. 1993, and references therein). At solar metallicity, this last component mainly produces the lighter s-process nuclei, at most up to Sr and Kr (Raiteri et al. 1993). In the case of ω Cen, if we assume that the s-elements are produced in the strong component, i.e. in a population of less massive asymptotic-giant-branch (AGB) stars (Busso et al. 1999, Ventura et al. 2009), we have to face a timescale discrepancy that makes hard to solve the entire puzzle (D'Antona et al. 2011). Indeed, these AGB have longer lifetimes than the more massive AGB stars, which are presumed responsible for the He enrichment and for Na-O anticorrelations. If, alternatively, the s-process elements are produced in the weak component by massive stars that explode as Type II Supernovae, it remains to be seen whether the models can produce elements as heavy as Ba and La in stellar environments characterized by the chemical abundances observed in ω Cen.

An important ingredient to understand the star-formation history of this poorly-understood GC is the determination of the relative ages of its stellar populations. Numerous studies based on CMD analysis combined with metallicity distribution of turnoff (TO) and SGB

stars have yielded conflicting results, suggesting age differences from less than 2 Gyr (Lee et al. 2005, Sollima et al. 2005, Calamida et al. 2009), up to 5 Gyrs (Villanova et al. 2007). Rapid-formation scenarios wherein the entire cluster could have formed within a few times 10^8 years have recently been suggested by D'Antona et al. (2011) and Valcarce & Catelan (2011).

Theoretical isochrones show that a variation of the total C+N+O abundance can have an effect on the GC ages obtained from CMD fitting. Therefore, the relative age-dating of the stellar populations hosted in the cluster would be severely affected by the presence of C+N+O differences among the ω Cen sub-populations (Cassisi et al. 2008, Ventura et al. 2009, Pietrinferni et al. 2009, D'Antona et al. 2009).

In an effort to shed light on these issues, in this paper we measure the overall C+N+O abundance in 77 RGB stars of ω Cen, which span nearly its entire metallicity range. The layout of this paper is as follows: in Section 2 we describe the data analysis; results are presented in Section 3, and their impact on the chemical enrichment scenario and the age measurements are discussed in Section 4 and Section 5, respectively; Section 6 is a summary of our results.

2. Observations and data reduction

Our data-set consists in a sample of 77 RGB stars observed with the FLAMES/GIRAFFE HR4 setup (program: 082.D-0424A). We also have, from Marino et al. (2011a), additional spectra for the same stars with different GIRAFFE setups, from which we have derived abundances for Fe, Na, O, and n-capture element La (75% s-process in the solar system, Simmerer et al. 2004). In Marino et al. (2011a) we provide meaurements also for Ba abundances, but here we prefer to use only La as representative of n-capture elements because Ba measurements are more uncertain, since the only analyzed Ba transition is a blend (see Marino et al. 2011a). We refer the reader to this paper for a more detailed description of the sample and the data reduction. Here we analyse, for 77 stars of the Marino et al. (2011a) sample, chemical abundances for carbon and nitrogen.

The HR4 setup covers the spectral range from ∼4188 to ∼4392 Å, providing a resolution R ∼20,000. The typical signal-to-noise ratio of the final combined spectra at the central wavelength of the spectral range is ∼80.

Our abundance analysis used the local thermodynamic equilibrium analysis code MOOG (Sneden 1973). Carbon was measured from spectral synthesis of the G-bandheads ($A^2\Delta - X^2\Pi$) near 4314 and 4323 Å. The nitrogen abundance was derived from synthesis of the CN

blue-system ($B^2\Sigma - X^2\Sigma$) bandhead at $\sim$4215 Å. The synthesis line list for the blue CN band is described in Hill et al. (2002). The line list for the CH band was provided by B. Plez (private communication). Synthetic spectra were employed by using Castelli & Kurucz (2004) models for effective temperatures (T_{eff}), gravities (log g), metallicities, and microturbolences (ξ_t) determined in Marino et al. (2011a). In computing the C abundance we used the previously determined O contents (Marino et al. 2011a), and for N, both observed C and O abundances needed to be employed. As an example, we show in Figure 1 the spectral synthesis for the CH and CN bands, and the O line for star #248664. For more details on the atmospheric-parameter determinations, and a discussion on related uncertainties, we refer to Marino et al. (2011a). Here, we focus on the C and N measurements.

The error analysis for C and N was performed by varying T_{eff}, log g, metallicity, and ξ_t for several stars, and redetermining the abundances. The parameters were varied by $\Delta T_{eff}=\pm100$ K, Δlog $g=\pm0.20$, $\Delta\xi_t=\pm0.10$ km/sec, and metallicity by 0.10 dex. In addition, the derived C abundance is dependent on the O abundance and therefore so is the N abundance, and the circulation of correlated errors tends to mimic the effects of CNO-cycle burning (e.g. Iben & Renzini 1983). Indeed, in the red giant atmospheres carbon is mainly present in the CO molecules, and in the molecular equilibrium an over-estimation in oxygen produces an over-estimation of carbon from the CH band, and viceversa. In the CN bands, a carbon over-estimation causes nitrogen to be under-estimated.

In the treatment of the internal errors for carbon, we then varied the oxygen abundance by ±0.10, and repeated the spectrum synthesis to determine the error introduced by uncertainties in the O abundances. These errors were then added in quadrature to the errors introduced by atmospheric parameters and yielded an overall error of $\sim \pm0.10$ dex to the [C/Fe] abundances. For nitrogen we varied both O and C, the latter by ±0.10 dex. We added these errors in quadrature with those introduced by the model atmosphere and estimated the internal uncertainty of the [N/Fe] values to be $\sim$0.20-0.30.

Carbon and nitrogen abundances for ω Cen RGB stars were determined by Brown & Wallerstein (1993; 6 stars), Norris & Da Costa (1995, 40 stars), and Stanford, Da Costa, & Norris (2010; 33 stars). A proper comparison with these studies cannot be made because there are no stars in common, however we note that our C and N values span a range similar to that of Brown & Wallerstein (1993) and Stanford et al. (2010). Possible systematic differences in C could not be excluded between our stars and those of Stanford et al., while systematically lower N abundances (of $\sim$0.50 dex) were found by Norris & Da Costa (1995).

In Marino et al. (2011a) we derived the O abundance from the line at 6300 Å by comparing our observations with synthetic spectra that had solar C and N. Here, we redetermine oxygen by adopting in the synthesis the measured N and C abundances. These improved

[O/Fe] measures are in good agreement with the previous measurements, with only few stars differing by more than 0.1 dex from the values in Marino et al. (2011a).
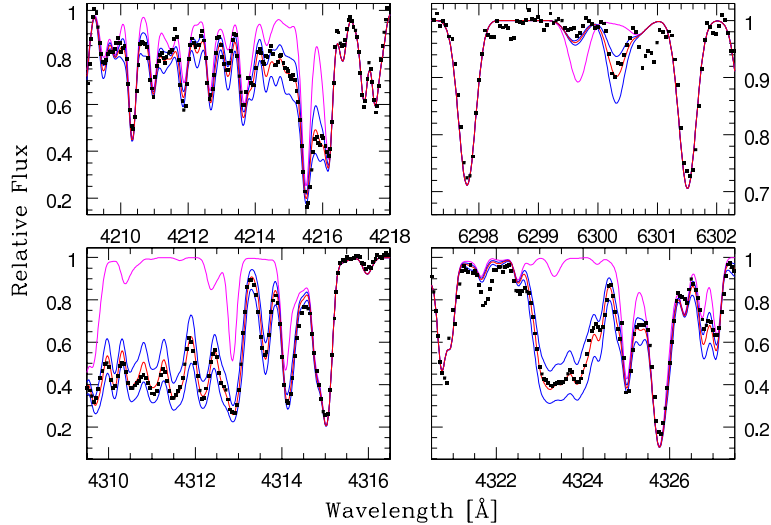

Fig. 1.— Observed and synthetic spectra around CH-bandheads (lower panels), CN-band (upper-left panel) and O line (upper-right panel) for the star #248664. The magenta line is the spectrum computed with no contribution from C, N, and O; the red line and blue lines are the best-fitting and the syntheses computed with abundance altered by ±0.25 dex from the best value, respectively.

3. Results

Figure 2 plots the abundances of C, N, and O (Tab. 1) measured in this paper and the Na measurements from Marino et al. (2011a). We observe large star-to-star variations in all of these elements, as has already observed in all the GCs studied to date. Carbon spans a range from [C/Fe]∼ −0.9 to [C/Fe]∼ +0.6. Most stars are C-depleted, but there is a population of stars with [C/Fe]>0.0. Nitrogen spans almost 2 dex, from [N/Fe]∼0.0 to stars with [N/Fe]∼1.8 dex. There is only one star (#214842) that is enhanced in both C and N (Figure 2, panel c).

Our results show the existence of well-defined patterns among C, N, O, and Na. A positive correlation is present between O and C, and between Na and N, and N anticorrelates with O (Figure 2, panels a, b, d). A C-N anticorrelation is not obvious (panel c), but it can be more easily recognizable by grouping stars on the basis of different Fe content, as will be
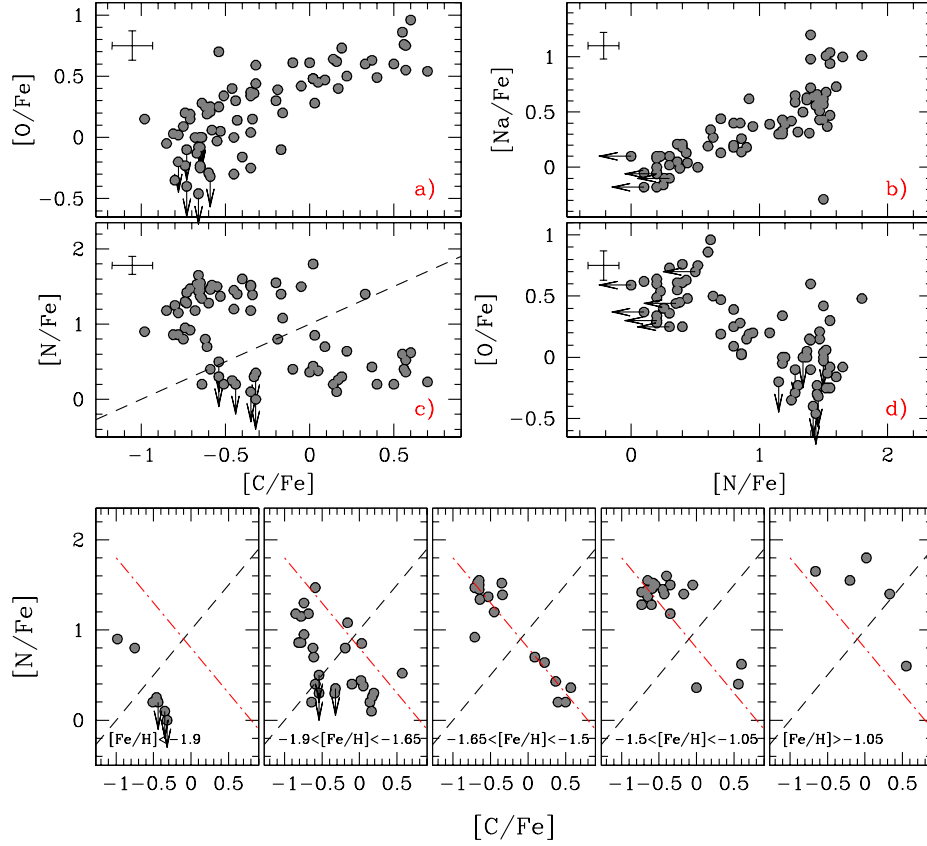
Fig. 2.— *Upper panels*: [N/Fe] and [O/Fe] vs. [C/Fe] (panels c, a), and [O/Fe] and [Na/Fe] vs. [N/Fe] (panels d, b). The dashed black line in panel (c) separates C-poor/N-rich stars from C-rich/N-poor. *Lower panels*: [N/Fe] vs. [C/Fe] in metallicity bins defined in Marino et al. (2011a). In each panel, the dashed black line is the same as in panel (c), the red dot-dashed line represents the "best-fit" line of constant [C/Fe]+[N/Fe] (=0.80) for the mid-metallicity stars.

discussed in Section 3.1. Such chemical patterns indicate the occurrence of high-temperature H-burning involving the CNO and NeNa cycles, and are consistent with prediction in Ventura & D'Antona (2009).

In the following sections we present the pattern of C, N, O abundances with [Fe/H] (Section 3.1) and with respect to the position of stars on the Na-O anticorrelation (Section 3.2) studied by Marino et al. (2011a).

ID	[C/Fe]	[N/Fe]	[O/Fe]
246266	−0.68	1.18	0.00
251010	−0.62	0.80	0.25
249334	−0.80	1.25	−0.35
248664	−0.19	0.80	0.39
240777	0.02	0.44	0.48
239549	−0.71	0.92	0.19

Table 1: Carbon, nitrogen and oxygen abundances ratios relative to iron for the analyzed stars The full table is only electronically available.

3.1. CNO pattern with [Fe/H]

Before discussing in detail the C, N, O patterns, we recall that ω Cen exhibits a large spread in [Fe/H], ranging from ~ -2.0 to ~ -0.7 dex. The iron distribution is multi-modal with distinct peaks at [Fe/H]$\sim -1.75, -1.60, -1.45, -1.00$, and there is a broad distribution of stars extending up to [Fe/H]~ -0.70 (Marino et al. 2011a). Although the existence of these multiple populations is clear, observational errors often prevent us from definitively establishing which individual stars belong to which population. Keeping this in mind, Marino et al. (2011a) defined six groups of stars with different iron abundances to investigate the Na-O anticorrelation for different metallicity groups (see their Figure 8).

In the lower panels of Figure 2, we perform a similar analysis for C versus N in the same metallicity bins defined in Marino et al. (2011a). Unfortunately, we do not have C and N measurements for the most metal-rich group, with [Fe/H]> -0.90, of Marino et al. (2011a). We see that the C-N anticorrelation is present across the entire range of metallicities. The dashed-black line in each panel (that is the same as in panel c) has been traced to arbitrarily separate the C-poor/N-rich population from the C-rich/N-poor one. The red dot-dashed line is the "best-fit" line of constant [C/Fe]+[N/Fe] for the mid-metallicity stars, that has been taken equal to 0.80.

It is worth noting that when we compare the relative location along the C-N anticorrelation with this line, it becomes evident that the average C abundance increases from lower to higher metallicities. The shape of the C-N anticorrelation for different metallicities is similar to that of the Na-O anticorrelation (Figure 8 of Marino et al. 2011a), with the most metal-rich groups hosting a larger fraction of N-rich (Na-rich, O-C-poor) stars. This behavior leads few stars, belonging to the metal richer group (e.g. #214842), to be enhanced both in C and N.

In the upper panels of Figure 3, we plot the individual carbon, nitrogen, and oxygen

abundances against iron. While [N/Fe] exhibits a mild correlation with [Fe/H], there is no clear correlation either between [C/Fe] and [Fe/H] or between [O/Fe] and [Fe/H]. A significant spread in light elements is present at all metallicities with [C/Fe], [N/Fe], and [O/Fe] spanning large ranges (more than 1 dex).

If, however, we instead plot the *total* [C+N+O] against [Fe/H], we find a correlation with a Pearson coefficient of 0.71. This is shown in panel (d) for the abundance relative to iron and in panel (e) for the total abundance. The red points show the averages over bins in [Fe/H] defined above. The vertical error bars correspond to the error in the mean related to the observed dispersion and the horizontal bars denote the boundaries of the [Fe/H] bins.

The representative error bar shown in the lower right of panels (d) and (e) comes from adding the individual C, N, and O errors in quadrature, and indicates that the error in the total [(C+N+O)/Fe] should be quite large ($\sim$0.3 dex). When we estimated the errors in these abundances, we made the assumption that the abundances were statistically independent. Given, though, that the C, N, and O abundances are correlated with each other, a more realistic estimate of the error might be derived empirically from the rms of the [(C+N+O)/Fe] within each metallicity bin. In this case, we find a rms ranging from 0.10 to 0.15 dex, and stars with intermediate metallicity ($-1.65 \leq$[Fe/H]< -1.05) have the largest rms.

The bottom panels of Figure 3 show the trends we have derived for ω Cen in the context of other clusters. M22 has stars with a range of metallicities (Marino et al. 2009), and these stars are shown as the green points, which happen to follow the ω Cen trend almost perfectly. On the other hand, the mono-metallic clusters for which we have data (NGC 6397, NGC 6752, M4, and 47 Tuc) do not follow this trend and, in general, show no discernible trend of [(C+N+O)/Fe] with metallicity.

3.2. CNO, Na and La abundances in the Na-O anticorrelation

To investigate how the studied chemical abundances behave for stars occupying a different location on the Na-O plane, we divided stars into two groups based on their location along the Na-O trend (Marino et al. 2011a). In normal mono-metallic clusters different generations of stars can be segregated in this way, and the Na-O groupings tend to have different C and N abundances, as can be seen in the case of M4 (Marino et al 2008, see their Fig 10). The situation in ω Cen has an added level of complexity, since the large variation in metallicity does not allow us to simply identify two (or more) populations via Na and O. Both Johnson & Pilachowski (2010) and Marino et al. (2011a) have shown that stars of both *first* and *second* generations are present across a large range of metallicities. Note that here

we extend the same nomenclature used for mono-metallic GCs to ω Cen and name first and second generation Na-poor/O-rich and Na-rich/O-poor stars respectively, whatever is their [Fe/H]. Of course, in the case of ω Cen this designation should not be taken literally, as stars of both groups are present in a large range in metallicity. We will therefore first follow the chemical patterns for the elements affected by p-captures (C, N, O, Na), n-capture elements (La), and C+N+O for the first generation alone, and then will examine the second generation.

In Figure 4 we represent in different colors our selected first and second generation stars on the Na-O anticorrelation from Marino et al. (2011a). The Na-poor/O-rich first generation (green open triangles) and the Na-rich/O-poor second generation stars (magenta open squares), have been arbitrarily selected by the dashed line. Similarly to what done in Figure 2, stars have been represented in different panels depending on their [Fe/H] bin. In each panel, the grey crosses represent the entire sample. The so selected first and second generation stars have been plotted in a O-La plane, as shown in Figure 5 (right panel). It is worth noting that in first generation stars [O/Fe] abundances correlate with [La/Fe], with the Pearson coefficient equal to 0.73. To quantify this correlation we have determined the mean [O/Fe] abundances for three La intervals spanned by first generation stars, whose sizes are indicated by the horizontal dark-green lines in Figure 5. The mean [O/Fe] values for the different Fe and La intervals are listed in Tab. 2, togheter with the rms and associated errors. In first stellar generation, some hints for a correlation may be present also among [O/Fe] and [Fe/H], as shown in the middle panel of Figure 5. In this case the O rise is more difficult to be claimed over observational errors and the mean [O/Fe] values in the selected metallicity bins (shown in dark-green in the middle panel of Figure 5) agree within a 3σ values.

| | [Fe/H] range | | | | | | [La/Fe] range | | |
	< -1.90	$-1.90/-1.65$	$-1.65/-1.50$	$-1.50/-1.05$	$-1.05/-0.95$	> -0.95	< -0.30	$-0.30/0.30$	> 0.30
[O/Fe]	0.41	0.45	0.50	0.62	0.64	$\cdots$	0.35	0.47	0.61
$\pm$	0.03	0.02	0.03	0.05	0.16	$\cdots$	0.01	0.02	0.03
σ	0.13	0.13	0.10	0.18	0.23	$\cdots$	0.08	0.10	0.15
# I-gen. stars	20	48	17	14	3	0	33	38	31

Table 2: Oxygen mean content for first generation stars in the Fe bins of Marino et al. (2011a), and for three intervals in [La/Fe].

We suggest some caution with the O trend in first generation stars, as we cannot fully exclude that it may be due to some unidentified systematics with iron. Johnson & Pilachowski (2010) do not find a trend of [O/Fe] with [Fe/H], but claim instead to find weak trends (~ 0.1 dex) in other α element ratios, such as [Ca/Fe] and [Si/Fe], which however are even weaker than our trend in [O/Fe]. Notice that such trend is detectable only among

first generation stars, as in second generation stars oxygen has been depleted by p-capture reactions.

As shown in the right panel of Figure 5, in first generation stars O increases in concert with the total CNO. At odds with first generation stars, the second generation ones (represented in magenta) do not appear to show any correlation with either La, Fe, and CNO, and occupy a spread region in all these abundance planes. Lanthanum abundance ratios follow a similar pattern for first and second generation stars as shown if Figure 6. This implies that the material out of which second generation stars have formed was not exposed to neutron sources (no additional n-captures besides those experienced by first generation stars) but only to p-captures. If AGB stars were responsible for the p-capture processing, this must have taken place in stars experiencing negligible third dredge-up, otherwise the material would have been further enriched in s-process elements.

In Figure 7 we summarize our results for C, N, O, and Na abundance ratios, that have been plotted as a function of [(C+N+O)/Fe], [Fe/H] and [La/Fe], for the first and second generation stars. As well as O, carbon increases as a function of the total CNO and [La/Fe], suggesting that C and O evolve in a similar way (though their errors are correlated).

At odds with C and O, neither N nor Na show any evidence for correlation with the total CNO abundance in first generation stars. However, the minimum values for these two elements may increase slightly with both Fe and La. N and Na display a much stronger trend with either the overall CNO, iron, and lanthanum for second generation stars, i.e. N and Na are higher for stars with higher CNO/Fe/La.

All the observed abundance pattern suggests that C and O from one side, and N and Na form the other, have undergone a similar processing in the evolution of the cluster. In addition, the first and second generation, selected on the basis of their Na and O content, appear to show well defined individual chemical trends along the overall observed range in metallicity.

Finally, the CNO increase among first generation stars is driven by the rise of O (and partly also of C), rather than N. As C and O increase with metallicity, more N could be produced by CNO cycling, and so in O-poor/Na-rich second generation stars both [N/Fe] and [Na/Fe] increase with metallicity. Figure 8 shows CNO vs. Fe separately for first and second generation stars, demonstrating the increase of CNO with Fe is common to both generations. The small offset ($< \sim 0.1$ dex) between the two generations may be real (due to part of CNO elements having been processed to heavier nuclei by p-captures), but we cannot fully exclude a slight systematic underestimate of N among second generation stars.

4. The formation and chemical enrichment of ω Cen

The interpretation of the photometric and spectroscopic evidences on the stellar populations of ω Cen in terms of its formation and evolution is posing formidable difficulties. In this Section we try to extract as much as possible from what the data themselves apparently demand.

Although there is photometric evidence for at least six different stellar populations in ω Cen (e.g., Bellini et al. 2010), we have distinguished a *first* and a *second generation* as made of those stars that do not or do show evidence for additional p-capture processing at high temperature, respectively. Thus, the *first generation* may represent a less complex case to interpret in terms of chemical evolution, with the *second generation* possibly arising from the AGB ejecta of the former one, as generally entertained.

4.1. Formation scenarios

We first explore a scenario in which the progenitor system to ω Cen has evolved as a single entity, in which the ISM was chemically homogeneous at each time. Thus, one can envisage the first generation to be the result of five or six successive bursts of star formation, with stars in each successive episodes being progressively enriched by nucleosynthesis products from core-collapse supernovae from the previous bursts. By construction, the first generation is made of stars which formed out of an ISM that was not yet polluted by p-capture products by AGB stars. This requirement sets an upper limit of 30-40 Myr between the first and the last burst, as later AGB stars would come at play.

Now, before the second generation starts to form most residual gas must be ejected from the system, thus allowing second generation stars being formed out of almost pure AGB ejecta. As emerging from all previous figures, second generation stars span the full metallicity range of ω Cen, which suggests that each episode of first generation formation has produced its own specific contribution to the second generation. Thus, after the five or six initial bursts of star formation, and the ejection of the residual gas, a similar series of bursts should have taken place out of gas from AGB ejecta being accumulated at the bottom of the potential well, via a series of cooling flows.

Also for this second generation series of bursts one can set a time limit to its duration, which comes from the necessity of avoiding the contamination by C/O>1 materials from carbon star ejecta, which should start some 2×10^8 yrs after the very first burst. Therefore, in this scenario all star formation episodes were confined to within $\sim 2 \times 10^8$ yrs. Of course, such a scenario with its complex series of events may require yet additional complications

to explain the presence of the Na-O anticorrelation among stars within different individual star formation episode of the second generation (i.e., within each [Fe/H] group). Even more complications may be required if the Na-O anticorrelation is due to partial mixing of AGB ejecta with pristine material as often invoked (e.g., D'Ercole et al. 2011, and references therein), though the origin of the diluting material remains to be understood. Five or six successive dilutions with *pristine* material would ask for an extremely contrived scenario. Alternatively, common-envelope ejecta from intermediate-mass binary stars may offer a less implausible option (Vanbeveren, Mennekens & De Greve 2011) but it remains to be seen if binaries can provide enough diluting material.

Moreover, as well known the original first stellar generation must have been much more massive than at present, if enough second generation stars formed from its AGB ejecta (e.g., Bekki & Norris 2006; Renzini 2008). This led to the hypothesis of a dwarf galaxy precursor of which ω Cen would be the stripped, remnant nucleus (e.g., Bekki & Freeman 2003; D'Ercole et al. 2010). In summary, in this scenario formation proceeds through a rapid series of star formation episodes (bursts), separated by just few Myrs in time, each followed by its own cooling flow made of AGB ejecta to form the second generation stars in a series of secondary bursts. Tidal stripping will then remove most of the original stellar mass of the system, leaving ω Cen as the bare nucleus of the original dwarf galaxy.

Alternatively, the several star formation episodes, rather than being sequential in time may have been separated in space, with each lump of matter having evolved (quasi)independently from the others, before merging together to make the cluster we observe today. In the original dwarf galaxy several high-density sites of star formation were active, each forming a proto globular cluster of first generation stars, with each of them later feeding the formation of its own second generation stars via a cooling flow of AGB-ejecta material. In turn, the densest part of the individual proto-clusters would merge together by dynamical friction and coalesce, thus forming a massive nucleus, to become ω Cen after all the rest of the dwarf galaxy is tidally stripped.

Difficult to say whether the former, *monolithic* scenario is more (or less) contrived than this *merger* one in which five or six proto-clusters evolve separately before coalescing together. Yet, the stellar population content of this most massive globular cluster in the Galaxy is so complex that we suspect no simple, straightforward model can be found for its formation. Eventually we must admit that we are still far from understanding this most puzzling cluster.

4.2. Chemical enrichment

The puzzle becomes even more difficult to compose when considering the specific chemical patterns exhibited by the stars in the cluster. Here we limit the discussion to the CNO elements.

In Figure 8 [(C+N+O)/Fe] appears to increase with [Fe/H] among first generation stars, a trend that is dominated by the increase of [O/Fe] since oxygen is the most abundant of the three elements. This is also indicated by the tight correlation between [(C+N+O)/Fe] and [O/Fe] seen in the right panel of Figure 6. The possible [O/Fe] increase with [Fe/H] among first generation stars, is contrary to the decreasing trend shown in all other environments. In fact, [O/Fe] decreases in lockstep with [Fe/H] in the Galactic thin disk, thick disk, bulge and halo (e.g., Bensby, Feltzing & Lundström 2004; Zoccali et al. 2006; Wheeler, Sneden & Truran 1989), a trend that is generally interpreted as due to a prompt enrichment of α-element by core collapse supernovae, followed by a slower iron enrichment by Type Ia supernovae (e.g., Matteucci & Greggio 1986). Moreover, values of [O/Fe] in excess of 0.5 are common among first generation stars, whereas they are extremely rare in any other environment. Therefore, also the *normal* population in ω Cen, the one not affected by proton captures, shows a unique chemical evolution history, not paralleled in any other known environment.

Thus, this classical scheme of chemical evolution may not apply to ω Cen's first generation, as we have that oxygen keeps increasing faster than iron, a clear evidence contrary to Type Ia supernovae playing a role in its enrichment. If so, one has to resort only on core collapse supernovae in trying to explain the [(C+N+O)/Fe] trend with [Fe/H]. This is not an easy task.

The existence of a broad range of metallicities among the first generation stars argues for enrichment and star formation having proceeded together in the progenitor object of ω Cen, though quite possibly as a series of successive *bursts*, as discussed in the previous subsection and indicated by the distinct photometric sequences present in this cluster (e.g., Bellini et al. 2010) paralleled by a multimodal distribution of [Fe/H] (e.g., Marino et al. 2011a).

In the scenario in which star formation proceeds with a series of bursts, the first successive episode would have experienced an enrichment due only to the most massive supernovae from the first episode, and the following ones an enrichment due to a broader and broader range of supernova masses. Thus a trend in [O/Fe] with [Fe/H] could be explained *if* the ratio of oxygen-to-iron yields from core collapse supernovae were a decreasing function of stellar mass, i.e., if low mass supernovae were to make more oxygen relative to iron, compared to

high mass supernovae.

Theoretical yields of oxygen and iron as a function of the initial mass of the supernova progenitor formally do not support this possibility (see e.g. Woosley & Weaver 1995; Limongi & Chieffi 2006; Kobayashi et al. 2006), but are sufficiently uncertain to leave this option *a priori* relatively viable. The main uncertainty comes from the iron yield as a function of stellar mass being poorly constrained by supernova models, mainly due to the difficulty in locating the *mass cut* between ejecta and compact remnant that typically lies just within the iron layer of the pre-supernova structure. Nevertheless, this scheme would require lower mass stars to dominate the oxygen production, whereas all supernova models agree in predicting an increase of the oxygen yield with stellar mass, at least up to $\sim 30\ M_\odot$, and in most models even beyond.

To explain the anomalous trend of [O/Fe] with [Fe/H] one may be tempted to appeal to the last resort of desperate situations, and invoke different IMFs for each successive episode of star formation, a very arbitrary and contrived scenario indeed. Moreover, note that this trend of increasing [O/Fe] with increase [Fe/H] does not extend to the highest metallicity group in ω Cen, corresponding to the *anomalous* RGB-a and MS-a sequences in the CMD (cf. old ref, Bellini et al. 2010), but here we have ascribed this whole metallicity group to the *p*-capture processed second generation.

In summary, even limiting ourselves to the *normal*, non *p*-capture processed, first generation, we have to admit our failure in providing an explanation for the observed [(C+N+O)/Fe] and [O/Fe] trends with [O/Fe].

5. CNO and age of ω Cen populations

The C+N+O abundance has a strong impact on the location of isochrones at the TO and SGB level, and therefore on age determinations. In order to estimate the effects of the large variation of the overall CNO among ω Cen's stellar populations on the age measurement, we have calculated stellar models by including a variety of assumptions on the C+N+O abundance and spanning a metallicity range suitable for the ω Cen stellar populations. The adopted physical inputs and numerical assumptions are the same as in Pietrinferni et al. (2009), which presents evolutionary computations accounting for a CNO enhancement of a factor of ~ 2 relative to the 'standard' α−enhanced mixture. A fully consistent set of α-enhanced isochrones with no CNO enhancement for various iron abundances (Pietrinferni et al. 2006), allows us to compare, in a fully homogeneous theoretical framework, CNO-enhanced and not-CNO-enhanced isochrones.

As expected, we find that, for a fixed TO and SGB brightness, the CNO-enhanced isochrones provide younger ages than isochrones corresponding to a canonical α-enhanced mixture (Pietrinferni et al. 2006): as a rule-of-thumb we found the ∂age/∂[CNO] ~ -3.3 Gyr dex^{-1}, regardless of the iron content. By accounting for the observed [CNO/Fe] abundance in ω Cen, we have estimated the difference between the age one would measure for each population by adopting appropriate CNO-enhanced isochrones and that obtained by using 'normally' $\alpha-$enhanced isochrones, i.e. neglecting the measure CNO enhancement. The overall effect is to decrease the age estimate for the higher metallicity stars. The age decrease ranges from $\sim$0.5 Gyr for stars with [Fe/H]~ -1.8 up to $\sim$2 Gyrs for the most metal-rich stars with [Fe/H]~ -1.0 (Figure 9), as listed in Table 3.

[Fe/H]	[(C+N+O)/Fe]	logϵ(C+N+O)	Δage(Gyr)
$-1.97<$[Fe/H]<-1.90	0.24$\pm$0.04	7.43$\pm$0.05	$-0.8\pm$0.1
$-1.90<$[Fe/H]<-1.65	0.34$\pm$0.03	7.69$\pm$0.04	$-1.1\pm$0.1
$-1.65<$[Fe/H]<-1.50	0.47$\pm$0.02	8.03$\pm$0.03	$-1.6\pm$0.1
$-1.50<$[Fe/H]<-1.05	0.48$\pm$0.04	8.24$\pm$0.05	$-1.6\pm$0.1
$-1.05<$[Fe/H]<-0.95	0.81$\pm$0.12	8.94$\pm$0.11	$-2.7\pm$0.4

Table 3: CNO contents and estimated age differences for the ω Cen [Fe/H] groups.

This result confirms that the measurement of relative ages of stellar populations in GCs requires accurate measurements of the overall C+N+O abundance. Indeed, it is well known that the double SGBs detected in NGC 1851, M22, 47 Tucanae (Milone et al. 2008, 2011, Anderson et al. 2009, Piotto 2009), can be interpreted in quite different ways, depending on the CNO content of the single populations. In particular, the faint SGB can be associated either with a stellar population significantly older than the stars in the bright SGB (up to 1 Gyr), or to a second generation, almost coeval with the brighter SGB (age differences of 100-200 Myr), but with enhanced CNO (Cassisi et al. 2008, Ventura et al. 2009). This scenario has received further support by recent findings in M22 by Marino et al. (2009, 2011b): this GC hosts two stellar groups with different s-element and CNO abundances, and, in addition, the two groups of CNO-rich and CNO-poor stars have also different iron abundances, in close analogy with ω Cen.

In NGC 1851, results on possible internal variations of C+N+O are contradicting (Yong et al. 2009, Villanova et al. 2010). However, theoretical models, properly accounting for photometric signatures of the chemical peculiarities observed in the cluster sub-populations as provided by Sbordone et al. (2011), suggest that in NGC 1851 only a C+N+O-enhanced second generation can satisfy all the observational constraints given by CMDs in various photometric bands (Milone et al. 2008, Han et al. 2009).

Many studies have attempted to reconstruct the evolutionary history of ω Cen, by determining relative ages among the different stellar sub-groups, but none has been able to account for variations in the overall C+N+O abundance. Considering the complexity of its SGB morphology, and of the metallicity distribution, and different assumptions regarding He enhancement among ω Cen populations, the relative ages for the various stellar populations as measured in different studies are quite different, ranging from a small or null age dispersion, as proposed by Sollima et al. (2005), to an age spread of the order of 2-3 Gyr (Hilker et al. 2004, Stanford et al. 2006) to 4 or more Gyr (Hughes & Wallerstein 2000, Hilker & Richtler 2000, Villanova et al. 2007).

It is beyond the scope of this paper to evaluate in detail how C+N+O abundances change the age-dating obtained in the multiple cited works. However, we can identify some general trends. By using the same α-enhanced isochrones adopted here, Villanova et al. (2007) found a large age difference ($\sim$5 Gyrs) among the ω Cen populations. Specifically they identify four groups of stars: (1) an old metal-poor group ([Fe/H]~ -1.7), (2) an old population of metal-rich stars ([Fe/H]~ -1.1), (3) a group of metal-intermediate young stars ([Fe/H]~ -1.4), about 1-2 Gyr younger than the old components, and (4) a young metal-poor group ([Fe/H]~ -1.7) up to $\sim$5 Gyr younger than the old populations. When accounting for the CNO overabundance and using appropriate CNO-enhanced isochrones, the age estimate of the metal-rich component in Villanova et al. should be decreased by $\sim$2 Gyrs. As a consequence, the metal-rich population is no longer coeval with the most metal-poor population, but is slightly younger. Similarly, due to its enhanced CNO content, the intermediate metallicity ([Fe/H]~ -1.4) population would be younger by $\sim$1 Gyr relative to the estimates given by these authors. On the other hand, the age difference between the two groups of old and young metal-poor stars should not change as they have the same iron and CNO content.

Hilker et al. (2004) and Stanford et al. (2006) suggest that ω Cen has experienced a prolonged star-formation of $\sim$2-4 Gyrs but, at odds with Villanova et al. (2007), with the most metal-rich stars being younger. Similar conclusions have been reached either by Hughes & Wallerstein (2000) and Hilker & Richtler (2000), who estimated that the more metal-rich stars were younger than the metal-poor ones by $\geq$3 Gyrs, and 3-6 Gyrs respectively. In the case of Hilker et al. (2004) and Stanford et al. (2006), we predict that CNO effects on the relative-age estimate could increase the duration of the star-formation in ω Cen up to $\sim$4-6 Gyrs.

Sollima et al. (2005) suggest that the global star-formation history of ω Cen should be confined to within $\sim$2 Gyrs, with the metal-poor population ([Fe/H]~ -1.7) representing the first and the major star-formation burst. Our results suggest that the ages of the metal-intermediate and metal-rich stars given by these authors could be over-estimated by $\sim$0.6 and

∼1.5 Gyrs, with respect to the metal-poor population. In any case, given their uncertainties of 2 Gyrs, these corrections do not change the main result of their work, e.g. the suggestion that ω Cen stellar populations formed in a short time period.

As mentioned above, the goal of this paper is not do a detailed analysis of previous age determinations. As discussed before there are contradicting results in recent literature. Our aim is simply to show that there is significant variation in the C+N+O content among ω Cen's populations that may easily change these datations. In addition to that caveat, it is worth noting that He enhancement is likely present in the O-poor, metal-rich stars. This occurrence should be taken into account when measuring the relative ages via isochrones fitting among the various sub-populations, since He affects the SGB shape (but not the luminosity level).

6.   Conclusion

In this paper, we have presented C, N, O abundances for 77 ω Cen RGB stars in the metallicity range $\sim -2.0 <$[Fe/H]< -0.9. We have coupled our results with the ones of our previous work on Na-O-La abundances presented in Marino et al. (2011a). From our analysis we found:

- a correlation between the total CNO and the iron abundance, with the most metal-rich population being enhanced by ∼0.5 dex in [(C+N+O)/Fe] relative to the most metal-poor one;

- O and C grows with [Fe/H] and [La/Fe] in the O-rich/Na-poor stars.

- stars selected on the basis of their position on the Na-O plane, show defined chemical patterns in their light elements C, N, O, and Na as a function CNO, Fe, and La, that allow us to distinguish between a *first* and a *second generation* of stars, each possibly resulting from a series of separate bursts of star formation.

- [La/Fe] correlates tightly with [Fe/H], following almost precisely the same trend regardless of the O/Na abundances.

In an attempt to make sense of this observational trends we have explored two (speculative) scenarios for the formation and evolution of this most puzzling object. In one option the system has evolved *monolithically*, i.e., remaining chemically homogeneous at each time. Thus, within less than $\sim 30 - 40$ Myrs a series of bursts of star formation each enriched in iron and α elements by core-collapse supernovae from the previous burst(s) would have been

followed each by a secondary burst of star formation originated from material ejected by AGB stars, heavily processed by p-captures. The formation of the whole stellar population inhabiting the cluster today would have taken less than $\sim 2 \times 10^8$ yrs. Alternatively, rather than sequential in time, such primary and secondary bursts of star formation would have taken place separately in space, before their products could merge at the bottom of the potential well. In both cases, secondary bursts would be fed via cooling flows made of AGB ejects, leading to more centrally concentrated *second generations*, which indeed appears to be so in this (and other) clusters (Sollima et al. 2005, Bellini et al. 2009, Johnson & Pilachowski 2010). We admit that both scenarios require a series of very contrived and *ad hoc* assumptions, yet the extraordinary complexity of ω Cen may not admit simple solutions.

The CNO abundance affects the determination of the relative ages of cluster subpopulations via isochrone fitting of the turnoff SGB region. In the light of our results, we have discussed this issue in the case of ω Cen by comparing isochrones with standard and with enhanced CNO, with the latter ones giving younger ages for the same turnoff luminosity. Although the determination of relative ages of ω Cen sub-populations is beyond the aims of our study, we argue that a trend in CNO/Fe can help reducing large age spread among the various sub-populations, as found by some studies in the literature.

REFERENCES

Anderson, A. J. 1997, Ph.D. Thesis,

Anderson, J., Piotto, G., King, I. R., Bedin, L. R., & Guhathakurta, P. 2009, ApJ, 697, L58

Bedin, L. R., Piotto, G., Anderson, J., Cassisi, S., King, I. R., Momany, Y., & Carraro, G. 2004, ApJ, 605, L125

Bekki, K., & Freeman, K. C. 2003, MNRAS, 346, L11

Bekki, K., & Norris, J. E. 2006, ApJ, 637, L109

Bellini, A., Piotto, G., Bedin, L. R., et al. 2009, A&A, 507, 1393

Bellini, A., Bedin, L. R., Piotto, G., et al. 2010, AJ, 140, 631

Bensby, T., Feltzing, S., & Lundström, I. 2004, A&A, 415, 155

Brown, J. A., & Wallerstein, G. 1993, AJ, 106, 133

Busso, M., Gallino, R., & Wasserburg, G. J. 1999, ARA&A, 37, 239

Calamida, A., Bono, G., Stetson, P. B., et al. 2009, ApJ, 706, 1277

Carretta, E., Gratton, R. G., Lucatello, S., Bragaglia, A., & Bonifacio, P. 2005, A&A, 433, 597

Cassisi, S., Salaris, M., Pietrinferni, A., Piotto, G., Milone, A. P., Bedin, L. R., & Anderson, J. 2008, ApJ, 672, L115

Cassisi, S., Salaris, M., Anderson, J., Piotto, G., Pietrinferni, A., Milone, A., Bellini, A., & Bedin, L. R. 2009, ApJ, 702, 1530

Castelli, F., & Kurucz, R. L. 2004, arXiv:astro-ph/0405087

D'Antona, F., Stetson, P. B., Ventura, P., Milone, A. P., Piotto, G., & Caloi, V. 2009, MNRAS, 399, L151

D'Antona, F., Caloi, V., & Ventura, P. 2010, MNRAS, 405, 2295

D'Antona, F., D'Ercole, A., Marino, A. F., et al. 2011, ApJ, 736, 5

D'Ercole, A., D'Antona, F., Ventura, P., Vesperini, E., & McMillan, S. L. W. 2010, MNRAS, 407, 854

Dupree, A. K., Strader, J., & Smith, G. H. 2011, ApJ, 728, 155

Han, S.-I., Lee, Y.-W., Joo, S.-J., Sohn, S. T., Yoon, S.-J., Kim, H.-S., & Lee, J.-W. 2009, ApJ, 707, L190

Hilker, M., & Richtler, T. 2000, A&A, 362, 895

Hilker, M., Kayser, A., Richtler, T., & Willemsen, P. 2004, A&A, 422, L9

Hill, V., et al. 2002, A&A, 387, 560

Hughes, J., & Wallerstein, G. 2000, AJ, 119, 1225

Ivans, I. I., Sneden, C., Kraft, R. P., Suntzeff, N. B., Smith, V. V., Langer, G. E., & Fulbright, J. P. 1999, AJ, 118, 1273

Iben, I., Jr., & Renzini, A. 1983, ARA&A, 21, 271

Johnson, C. I., & Pilachowski, C. A. 2010, ApJ, 722, 1373

Kobayashi, C., Umeda, H., Nomoto, K., Tominaga, N., & Ohkubo, T. 2006, ApJ, 653, 1145

Lee, Y.-W., Joo, J.-M., Sohn, Y.-J., Rey, S.-C., Lee, H.-C., & Walker, A. R. 1999, Nature, 402, 55

Lee, Y.-W., Joo, S.-J., Han, S.-I., et al. 2005, ApJ, 621, L57

Limongi, M., & Chieffi, A. 2006, ApJ, 647, 483

Marino, A. F., Villanova, S., Piotto, G., Milone, A. P., Momany, Y., Bedin, L. R., & Medling, A. M. 2008, A&A, 490, 625

Marino, A. F., Milone, A. P., Piotto, G., Villanova, S., Bedin, L. R., Bellini, A., & Renzini, A. 2009, A&A, 505, 1099

Marino, A. F., et al. 2011a, ApJ, 731, 64

Marino, A. F., et al. 2011b, A&A, 532, A8

Matteucci, F., & Greggio, L. 1986, A&A, 154, 279

Milone, A. P., et al. 2008, ApJ, 673, 241

Milone, A. P., Piotto, G., Bedin, L. R., et al. 2011, arXiv:1109.0900

Norris, J. E., Freeman, K. C., & Mighell, K. J. 1996, ApJ, 462, 241

Norris, J. E., & Da Costa, G. S. 1995, ApJ, 447, 680

Norris, J. E. 2004, ApJ, 612, L25

Pancino, E., Ferraro, F. R., Bellazzini, M., Piotto, G., & Zoccali, M. 2000, ApJ, 534, L83

Pietrinferni, A., Cassisi, S., Salaris, M., & Castelli, F. 2006, ApJ, 642, 797

Pietrinferni, A., Cassisi, S., Salaris, M., Percival, S., & Ferguson, J. W. 2009, ApJ, 697, 275

Piotto, G., et al. 2005, ApJ, 621, 777

Piotto, G. 2009, IAU Symposium, 258, 233

Raiteri, C. M., Gallino, R., Busso, M., Neuberger, D., & Kaeppeler, F. 1993, ApJ, 419, 207

Renzini, A. 2008, MNRAS, 391, 354

Sbordone, L., Salaris, M., Weiss, A., & Cassisi, S. 2011, A&A, 534, A9

Simmerer, J., Sneden, C., Cowan, J. J., Collier, J., Woolf, V. M., & Lawler, J. E. 2004, ApJ, 617, 1091

Smith, V. V., Suntzeff, N. B., Cunha, K., Gallino, R., Busso, M., Lambert, D. L., & Straniero, O. 2000, AJ, 119, 1239

Sollima, A., Pancino, E., Ferraro, F. R., Bellazzini, M., Straniero, O., & Pasquini, L. 2005, ApJ, 634, 332

Sneden, C. A. 1973, Ph.D. Thesis

Stanford, L. M., Da Costa, G. S., Norris, J. E., & Cannon, R. D. 2006, ApJ, 647, 1075

Stanford, L. M., Da Costa, G. S., & Norris, J. E. 2010, ApJ, 714, 1001

Suntzeff, N. B., & Kraft, R. P. 1996, AJ, 111, 1913

Valcarce, A. A. R., & Catelan, M. 2011, arXiv:1106.6082

Vanbeveren, D., Mennekens, N., & De Greve, J. P. 2011, arXiv:1109.2713

Ventura, P., & D'Antona, F. 2009, A&A, 499, 835

Ventura, P., Caloi, V., D'Antona, F., Ferguson, J., Milone, A., & Piotto, G. P. 2009, MNRAS, 399, 934

Villanova, S., et al. 2007, ApJ, 663, 296

Villanova, S., Geisler, D., & Piotto, G. 2010, ApJ, 722, L18

Wheeler, J. C., Sneden, C., & Truran, J. W., Jr. 1989, ARA&A, 27, 279

Woosley, S. E., & Weaver, T. A. 1995, ApJS, 101, 181

Yong, D., Grundahl, F., D'Antona, F., Karakas, A. I., Lattanzio, J. C., & Norris, J. E. 2009, ApJ, 695, L62

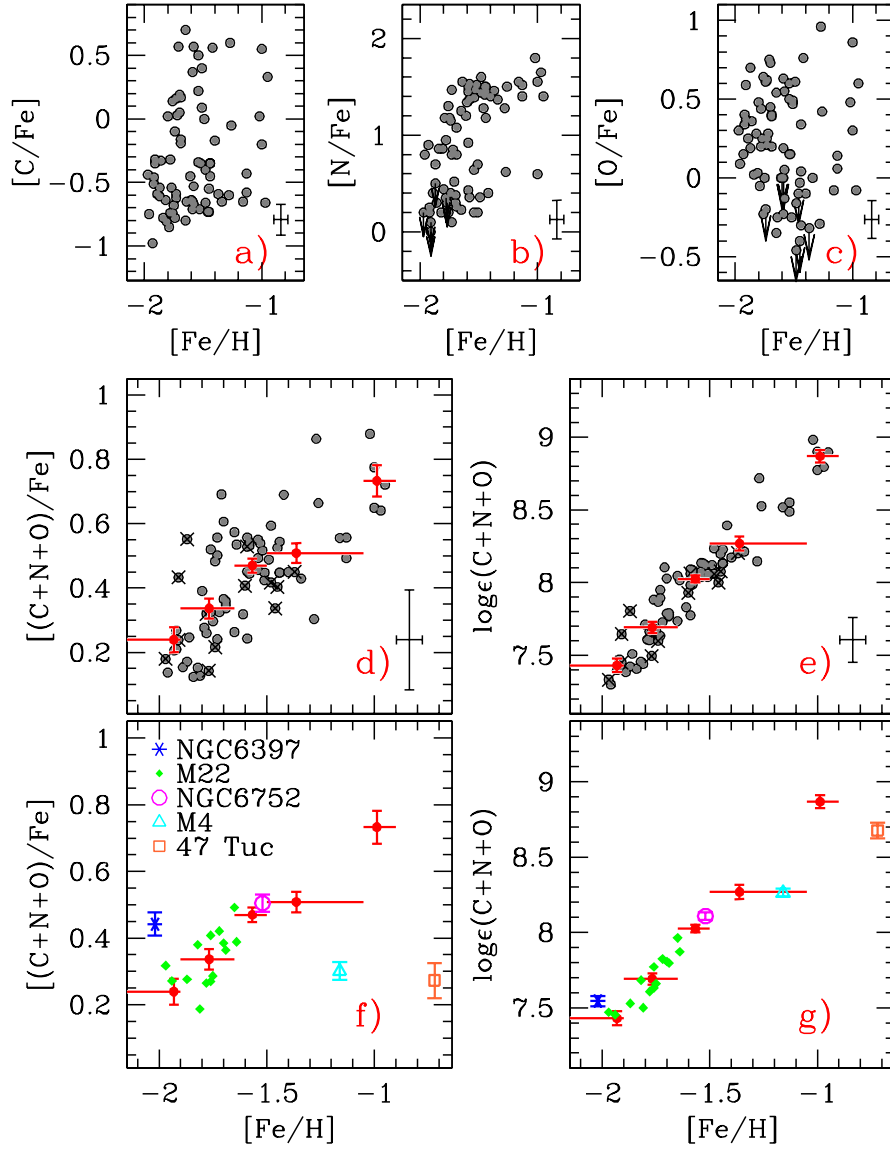Zoccali, M., Lecureur, A., Barbuy, B., et al. 2006, A&A, 457, L1

Fig. 3.— *Upper panels*: [C/Fe], [N/Fe], and [O/Fe] vs. [Fe/H]. *Middle panels*: [(C+N+O)/Fe] and logε(C+N+O) vs. [Fe/H]. Stars with upper limits for O or N abundances are represented as grey crosses. Red points represent the average C+N+O content in the metallicity intervals spanned by the horizontal red bars. Vertical bars are the errors associated with the mean values. *Lower panels*: Average [(C+N+O)/Fe] vs. iron for the GCs quoted in the inset compared with the ω Cen CNO mean values (red points) of panels *d* and *e*. Data for the mono-metallicity GCs are from Ivans et al. (1999) for M4, and Carretta et al. (2005) for 47 Tuc, NGC 6752, NGC 6397. Data for M22 are from Marino et al. (2011b).
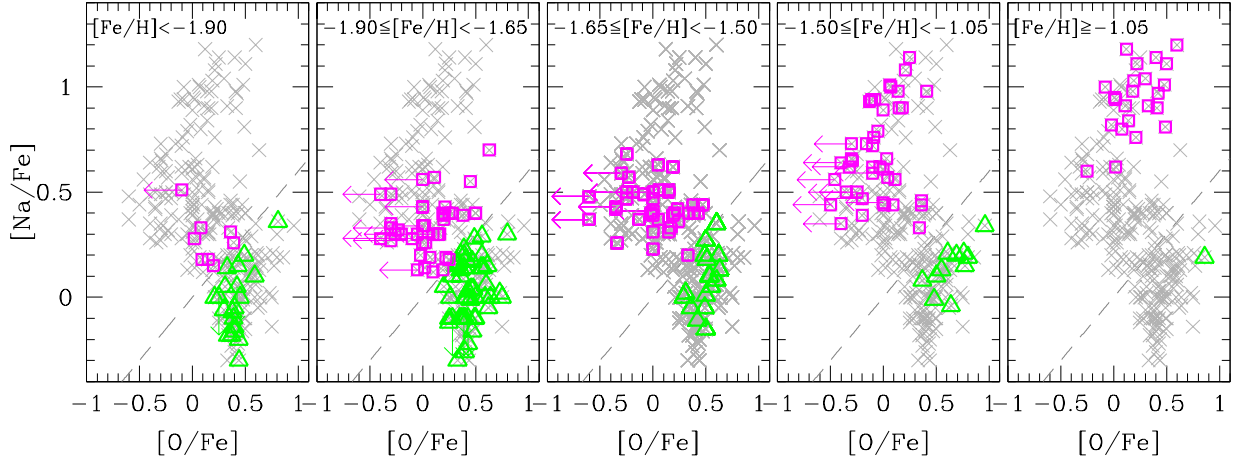
Fig. 4.— Our adopted division of stars in O-rich/Na-poor (*first generation*) and O-poor/Na-rich (*second generation*) has been represented in the Na-O plane for each metallicity bin, as quoted in the insets. The dashed line separates the selected first generation stars represented by green triangles, from the selected second generation stars represented by magenta squares. Gray crosses in each panel represent the entire sample analysed by Marino et al. (2011a).
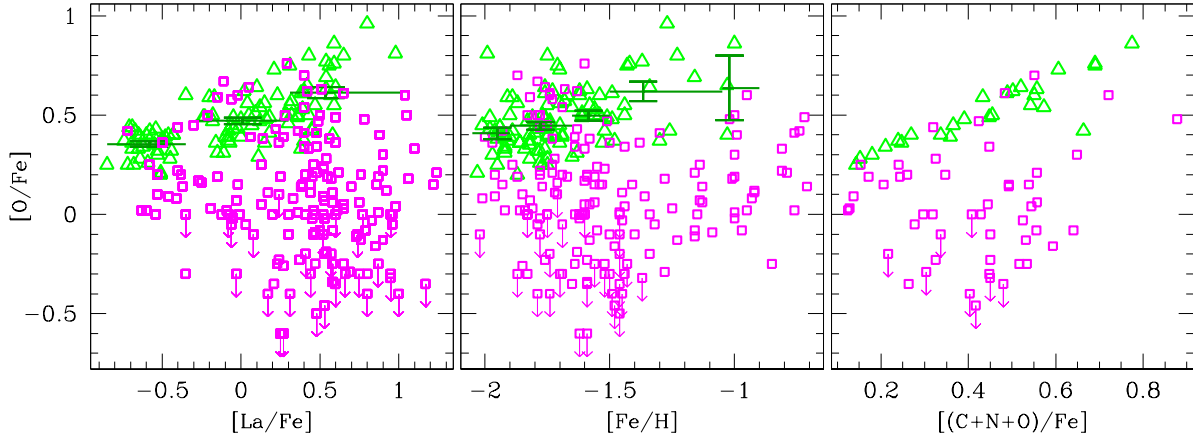

Fig. 5.— O abundance ratios as a function of [La/Fe], [Fe/H] and [(C+N+O)/Fe]. Symbols are as in Figure 4. The dark green vertical error bars represent the error associated with the mean [O/Fe] abundance in different intervals in [La/Fe] and [Fe/H] delimited by the horizontal line.
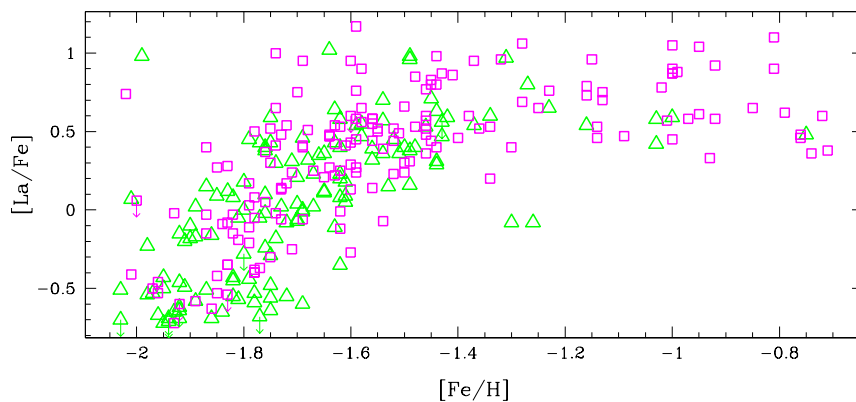
Fig. 6.— [La/Fe] as a function of [Fe/H]. Symbols are as in Figure 4.
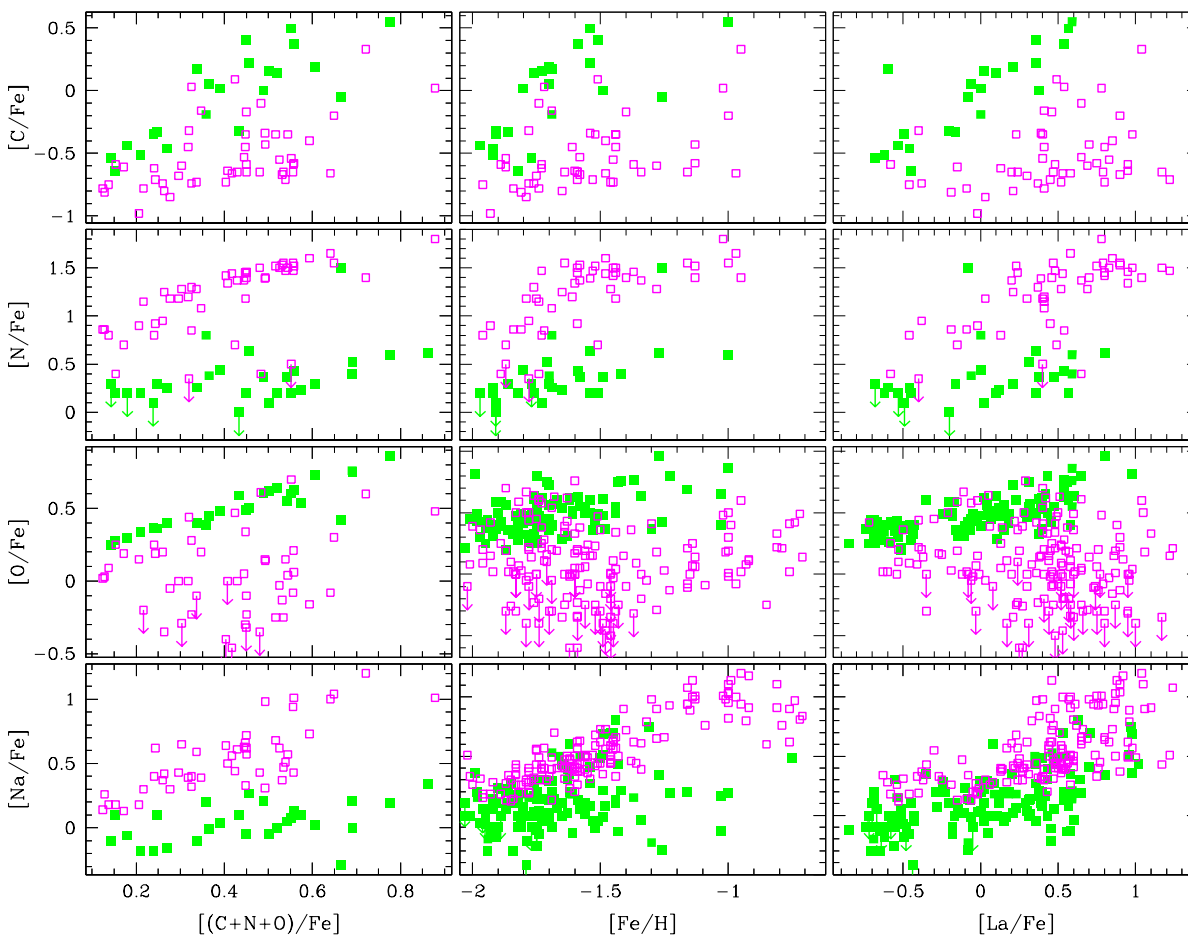

Fig. 7.— C, N, O, and Na abundance ratios as a function of [(C+N+O)/Fe], [Fe/H] and [La/Fe]. Symbols are as in Figure 4.
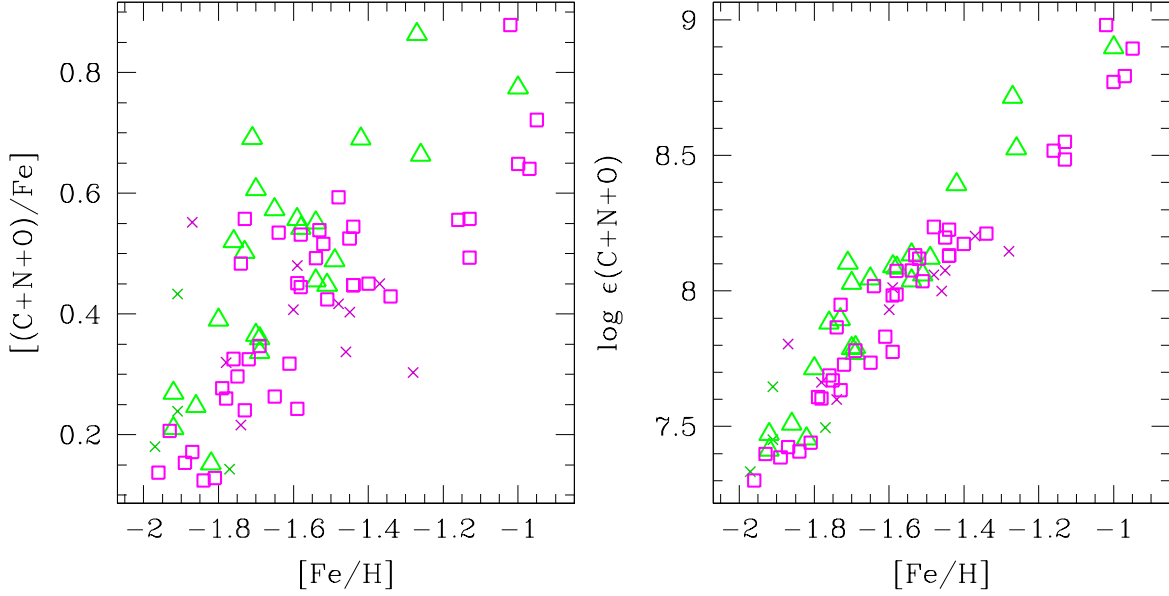
Fig. 8.— CNO relative to Fe and logϵ(CNO) as a function of [Fe/H]. Symbols are as in Figure 4. Crosses mark stars for which we have only an upper limit for N or O.
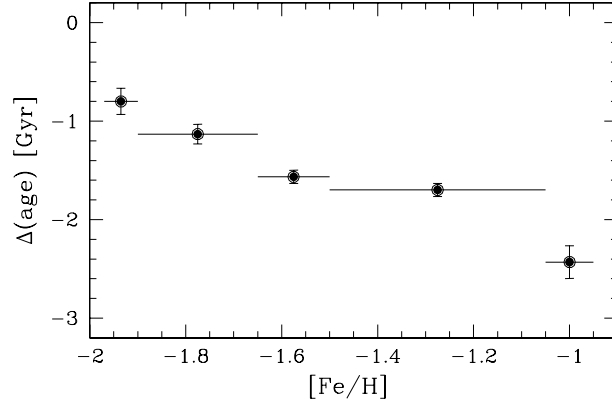

Fig. 9.— Age difference for each ω Cen sub-population, between the estimates based on CNO-enhanced isochrones and on the actual C+N+O abundances, and the measurements provided by not CNO-enhanced isochrones.